Damage detection of offshore platforms using acoustic emission analysis

Guijie Liu,[1,a)] Shirui Wang,[1] Yingchun Xie,[1] Xiaojie Tian,[1] Dingxin Leng,[1]
Reza Malekain,[2] and Zhixiong Li[3,a)]
[1]*School of Engineering & Key Laboratory of Ocean Engineering of Shandong Province, Ocean University of China, Qingdao 266100, China*
[2]*Department of Electrical, Electronic and Computer Engineering, University of Pretoria, Pretoria 0002, South Africa*
[3]*School of Mechanical, Materials, Mechatronic and Biomedical Engineering, University of Wollongong, Wollongong, NSW 2522, Australia*

(Received 25 August 2018; accepted 1 November 2018; published online 20 November 2018)

This paper aims to detect the structure damage in KT type jacket offshore platforms using acoustic emission analysis. Experimental investigation has been implemented to analyze the transmission characteristics, attenuation law, and source localization of the acoustic emission signals. The range of energy attenuation coefficient α and the signal amplitude attenuation law were obtained from experimental data. Hence, the layout of acoustic emission sensors was optimized based on the energy attenuation to achieve online damage monitoring for KT-jacket platforms. In order to validate the performance of the optimized sensor layout, another experimental test was conducted on the designed KT-jacket offshore platform to locate the acoustic emission sources. The test results demonstrate that a positioning error of 8 mm or below can be obtained using the optimized sensor layout, and the number of sensors can be reduced by 80% compared with that of the theoretical layout. As a result, the optimized sensor layout enables efficient and effective damage detection for KT-jacket offshore platforms. *Published by AIP Publishing.* https://doi.org/10.1063/1.5053735

I. INTRODUCTION

Offshore platforms are subject to extreme loads during their long service lives, resulting in common structural damages such as fatigues, cracks, and corrosion.[1] It is reported that 80% severe structure damages in offshore platforms are caused by fatigue crack on tube joints.[1–3] Therefore, online monitoring of fatigue cracks is of important significance to prevent failures of offshore platforms.[4,5] Due to deep sea environment, it is impossible/difficult to perform visual inspection on structural damages of offshore platforms. Alternatively, the damage detection can be carried out by monitoring the changes of modal characteristics in the offshore structures.[6] In addition, the ultrasonic and radiograph detection techniques are also employed to inspect the potential structure damages.

Recently, the acoustic emission has become the most promising tool for damage detection of offshore platforms. The acoustic sources of complicated structures can be located using two positioning algorithms. One is the spatial spectrum estimation, and the other is the time delay estimation. Schmidt[7] proposed the multiple signal classification (MUSIC) algorithm for sound signal processing. MUSIC enables simultaneous direction finding of either multiple or instant short signals with high precision. However, MUSIC is mainly used for spatial spectrum estimation of narrow-band signal and is limited in processing wide-band signals like acoustic emission signal due to heavy computation cost. Omologo and Svaizer[8] put forward a cross-spectrum-phase time delay estimation algorithm, which can locate the sound source in three-dimension (3D) space under different noise and echo conditions. Yegnanarayana *et al.*[9] divided two sound signals generated by the same source into equal-length fragments and extracted their short-time spectrum characteristics. On this basis, the time delay estimation to each fragment was conducted to achieve better positioning effect than that of the generalized cross correlation. Jia *et al.*[10] calculated azimuth and slope of each sound sensor in 3D space using the time delay estimation to locate the sound source according to geometric positions. Previous researches demonstrate that the time delay estimation is more suitable for acoustic emission processing than the spatial spectrum estimation. The time domain correlation of multi-sensory signals is usually calculated to determine the spatial position of the sound source. However, in practice, the identification accuracy of sound sources is subject to heavy distortion of the acoustic emission signals and the sensor noise.[11,12]

In order to accurately determine the sound source localization, it is critical to optimize the sensor layout in the online damage monitoring system for offshore platforms.[13–15] Although independent 3D positioning monitoring of all joints of offshore platform structures could improve monitoring precision, it requires a large number of sensors and thereby produces poor economic efficiency.[16,17] Considering practical environment and economical efficiency,[18,19] only limited number of acoustic emission sensors is expected to be installed on suitable positions of the offshore platforms. It is an important premise to propose a practical sensor layout as improper layout will affect parameter identification accuracy,

[a)]Authors to whom correspondence should be addressed: Guijie Liu (liuguijie@ouc.edu.cn) and Zhixiong Li (zhixiong.li@ieee.org)

thus decreasing the detection accuracy of the online monitoring system for offshore platform damage. Sensor layout optimization should meet the following constrains: (1) the sensor measurements are able to contain structural information to the maximum extent, and (2) the measurements are sensitive enough to the changes of structural health state. However, because the layout of acoustic emission sensors is closely related with the materials and scales of the structures,[20–23] it is a challenging task to optimize the sensor layout for the practical use of damage detection. Very limited work has been found in the literature to address this challenge.

In order to bridge the research gap in sensor layout optimization for online monitoring of offshore platform damage, theoretical and experimental analyses have been conducted to optimized acoustic emission sensor layout using a special designed offshore platform with 12 KT jackets. The energy attenuation coefficient α and attenuation law of the sensory signal amplitude were obtained through experimental data. An optimized layout algorithm of acoustic emission sensors for online monitoring of fatigue crack was proposed. The experimental evaluation shows the effectiveness of the optimized sensor layout for acoustic emission source identification.

II. THE PROPOSAL METHOD

A. Energy attenuation experiment

1. Main legs of KT-Jacket offshore platform structure

An experimental model of a KT jacket offshore platform (scale ratio: 1:100) was designed and manufactured based on the geometric similarity theory (see Fig. 1). The platform was welded by plain round bars, and each 2 bars were fixed with a joint. The main frame consists of four pieces of leg reinforcing bars, three layers of horizontal supporting reinforcing bars, and one roof plate. The total height was 2430 mm, the length and width of the base legs were 682 and 445 mm, respectively. The diameter of the main legs was 18 mm, the horizontal supporting diameter was 10 mm, and the thickness of the roof plate was 2 mm.

The PXWAE digital full-waveform acoustic emission detector made by Beijing Pengxiang Science and Technology Co., Ltd was used in the experiments to record the structure acoustic emissions (see Fig. 2). According to the requirements of American Society for Testing and Materials (ASTM), the wave attenuation test for the acoustic emission signal should be implemented by using φ = 0.5 mm HB pencil lead. The pencil lead was extended by 2.5 mm and then was broken up when forming a 30° angle to the component surface. PXR15 acoustic emission sensors were used in the pencil lead test. The center frequency of PXR15 was 150 kHz. PXPAIV low-noise amplifier with 40 dB gain was used as the preamplifier. The main amplifier gain of PXWAE was 0 dB. Good sound coupling between the sensor and test surfaces is the prerequisite of sensor installation. Loose coatings, oxide skin, rough surface, oil stain, or excessive materials on test samples were removed before the test. The sensor contact surface was filled with appropriate amount of coupling agent, and the coupling layer was made thin enough to ensure good measuring sensitivity. The magnet bases were used to fix the sensors on the offshore platform.

FIG. 1. The designed KT-jacket offshore platform structure.

For the convenience of experimental result analysis and intuitive representation of attenuation law, the wave attenuation test was conducted on the main leg. Figure 3 shows the breaking positions of the pencil lead. An acoustic emission sensor was fixed on the left end of the main leg and 19 lead-breaking positions were chosen with an interval of 0.1 m to

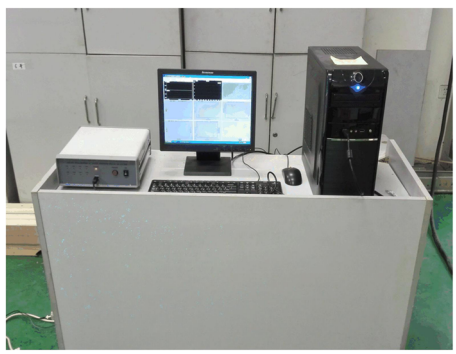

FIG. 2. The acoustic emission signal acquisition system.

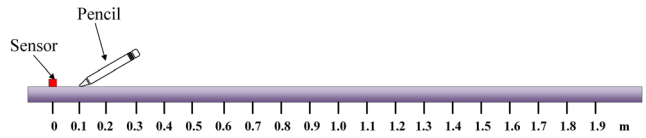

FIG. 3. Lead-breaking positions on the main leg for energy attenuation experiment.

each other, starting from the sensor position. The wave attenuation test was repeated for six times, and the mean of the sensor measurements was used.

The test results are shown in Figs. 4 and 5. The amplitudes and the energy of the collected acoustic emission signals were displayed.

It can be seen from Figs. 4 and 5 that both the amplitude and energy of acoustic emission signals declined when transmitting in the main leg, but presented small fluctuations. It is important to note that obvious amplitude and energy concentration at 0.5 m position can be observed in all tests. In addition, the amplitude/energy decreased continuously from 0.1 to 0.5 m and then fluctuated from 0.5 to 1.2 m and decreased after 1.2 m. This is because when the distance between the acoustic emission source and the sensor is smaller than 0.5 m in the jacket offshore platform, the sensor may miss some signal components, resulting in energy attenuation within a small range. As this distance increases to 0.5-1.2 m, acoustic emission waves may superpose in medium because of reflection and diffraction, leading to signal energy growth and fluctuation. After 1.2 m in distance, the signal energy of the acoustic emission obeyed the attenuation law.

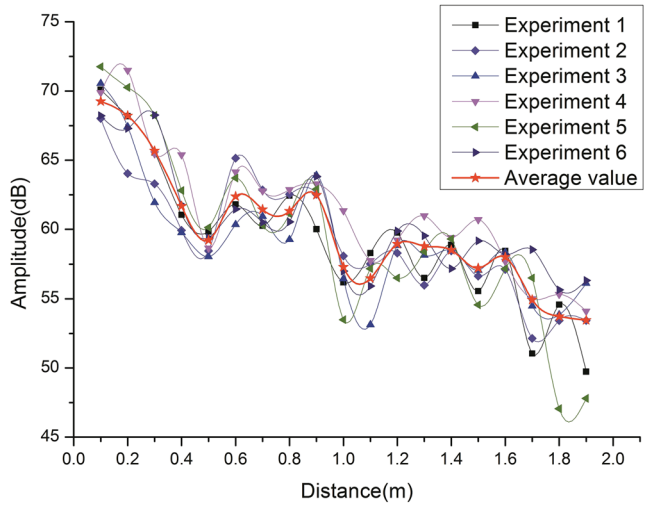

FIG. 4. Amplitude-distance attenuation curves.

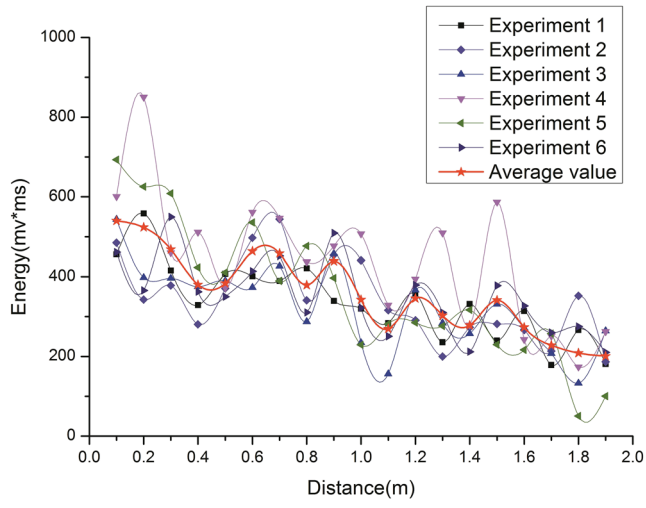

FIG. 5. Energy-distance attenuation curves.

The results of the wave attenuation tests show that the acoustic emission technique is applicable to crack detection on KT jacket offshore platforms. Influenced by the material type, structural shape, and scale, the acoustic emission wave transmission in actual structural medium is very complicated. Hence, it is important to investigate the attenuation characteristics in the damage detection to optimize the sensor layout.

2. Supporting rods of KT-jacket offshore platform structure

Figure 6 describes the joint details in the KT-jacket offshore platform. Rods 1 and 3 are the lateral supports, rods 2 and 5 are the main support of the cross section, and rod 4 is the lateral support of the cross section. In order to investigate the attenuation characteristics of the joint, the acoustic emission sensor #1 was fixed on the joint to measure the energy released by the lead-breaking source and the sensor #2 was, respectively, fixed on the rods to measure the signal energy in different transmission paths. In the attenuation tests, sensor #2 was put at different positions on each rod. On this basis, the energy attenuation characteristics of the supporting rods were analyzed.

The attenuation test at each rod was repeated for three times, and the mean of the sensor measurements in the three tests was used. Define E_s as the energy of the acoustic emission source collected by sensor #1 and E_i as signal energy collected by sensor #2. The energy ratio of the two sensors is E_i/E_s. Figure 7 shows the experimental results. Due to reflection and diffraction effect of the acoustic emission, the lead-break energy received by sensors #2 at rod 3 with long-distance was stronger than that with short-distance. For the other four rods, the energy attenuated continuously as the distance increased, which was in consistent with the theoretical analysis. However, the attenuation law on different

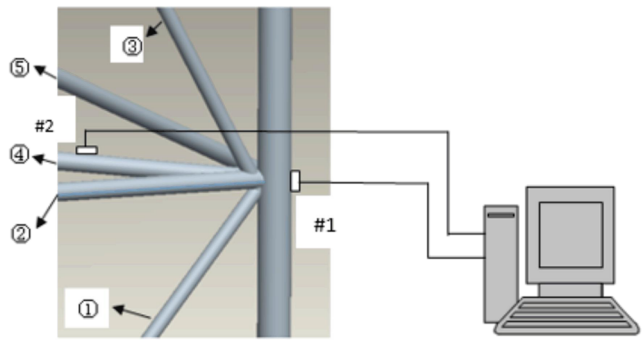

FIG. 6. Sensor layout on supporting rods.

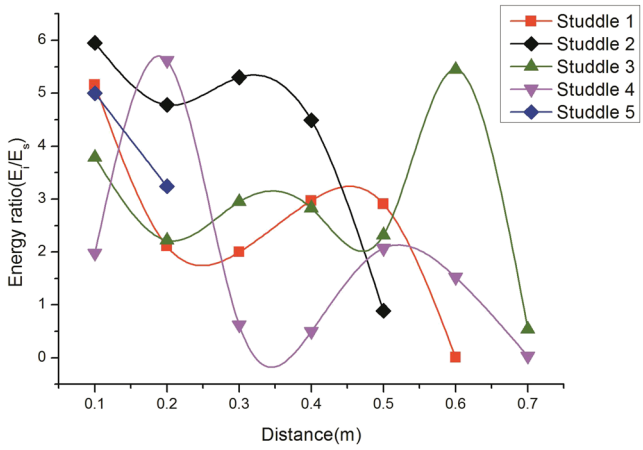

FIG. 7. Energy ratio-distance curve on supporting rods.

rods varied due to different diameters and directions. It is difficult to obtain a unified attenuation law. However, it should note that E_i/E_s at 0.5 m of rods 1, 3, and 4 presented evident concentration to value 2, while E_i/E_s at 0.5 m of rod 2 was about 1. These observations can be used for practical damage detection. Because rod 5 is too short, we did not discover valuable attenuation information.

The energy attenuation transmission model of the acoustic emission signal can be described as a function of the distance to the acoustic emission source.[24] Assume that a coordinate of the sound source is r and a sensor array of N sensors is used to measure the sound transmission signal. The position coordinates of the ith sensor is expressed as r_i, (i = 1, 2, . . ., N). The acoustic emission energy measured by the ith sensor is

$$E_i(t) = g_i \frac{E_s(t - t_i)}{|r(t - t_i) - r_i|^{\alpha}} + \varepsilon_i(t), \tag{1}$$

where t_i is the time delay when the acoustic emission transmits to the ith sensor; $E_s(t - t_i)$ is the energy emitted by the source at the position of the ith sensor, and $r(t - t_i)$ is the corresponding coordinate of the source; r_i is the coordinate of the ith sensor, and g_i is the gain coefficient of the ith sensor; α ($\approx$2) is the energy attenuation coefficient; and $\varepsilon_i(t)$ is the collaborative effect of the model cumulative error caused by observation noise. Neglecting $\varepsilon_i(t)$, Eq. (1) can be reduced as

$$|r(t - t_i) - r_i|^{\alpha} = g_i \frac{E_s(t - t_i)}{E_i(t)}. \tag{2}$$

Then, the energy attenuation coefficient α can be deduced by

$$\alpha = \log_{|r(t-t_i)-r_i|} g_i \frac{E_s(t-t_i)}{E_i(t)}. \tag{3}$$

Since the sensors used the same preamplifier, the effect of the gain coefficient g_i can be neglected. Thus, Eq. (3) can be rewritten as

$$\alpha = \log_{|r(t-t_i)-r_i|} \frac{E_s(t-t_i)}{E_i(t)}. \tag{4}$$

The energy attenuation coefficients calculated based on Eq. (4) using the experimental data are listed in Table I.

It can be seen in Table I that the wave transmission attenuation in practice is more complicated than that in theoretical analysis because α at different points of the jacket offshore platform varied significantly; even though the distance to the sound source was the same. This is probably because the structural medium is not complete elastic so that wave decays at a certain degree due to geometric factors (i.e., with the expansion of wave surface, the distribution volume of the elastic wave will increase, thus decreasing energy per unit volume). Moreover, wave transmission is influenced by various factors, such as the structure shape and scale. It should be also noticed that in Table I the α values of rods 1, 3 and 4 with 0.5 m distance are closer to the theoretical value 2 compared to those at other positions. Therefore, the following research will focus on the 0.5 m position.

TABLE I. Energy attenuation coefficients.

Distance (m)	Rod 1	Rod 2	Rod 3	Rod 4	Rod 5
0.1	0.71	0.77	0.58	0.30	0.70
0.2	0.46	0.97	0.50	1.07	0.73
0.3	0.57	1.38	0.90	−0.40	NA
0.4	1.19	1.64	1.14	−0.77	NA
0.5	1.54	−0.17	1.21	1.05	NA
0.6	−8.37	NA	3.32	0.82	NA
0.7	NA	NA	−1.75	−10.28	NA

B. Sensor layout optimization

Cracks often appear and propagate randomly on the jacket offshore platforms. Any part of the platform structure may be a potential acoustic emission source of cracks. As a result, it is very difficult to make an optimal arrangement of acoustic emission sensors. To this end, a hypothesis that assumes equal probability of acoustic emission cracks in the structure joints is made in the sensor layout optimization. Since the tube joint is the most important but the most frequently broken component in the KT jacket offshore platforms,[25–27] this paper considers the sensor layout optimization for tube joints.

According to the relationship between the vibration direction and the acoustic transmission direction, acoustic emission wave may transmit in different modes such as the longitudinal wave, shear wave, Rayleigh wave, and plate wave. Reflection, refraction, and mode conversion will take place when the wave reaching different medium interfaces.[28] If acoustic emission wave is generated from a single source in a semi-infinite solid body, the transmission of longitudinal wave, shear wave. or Rayleigh wave will follow closely to one point on the surface. Interaction between different transmission models will complicate the wave transmission (see Fig. 8).

The transmission mode of acoustic emission wave in the thick steel plate is shown in Fig. 9. During the transmission, the acoustic wave will reflect many times between the two medium interfaces and each reflection will excite the mode conversion. It also will generate plate wave with a wavelength almost equal to the plate thickness. As a result, in practice, the wave transmission of acoustic emission is more complicated than that in ideal medium.

According to the energy attenuation characteristics of the acoustic emission signals in the experimental tests,

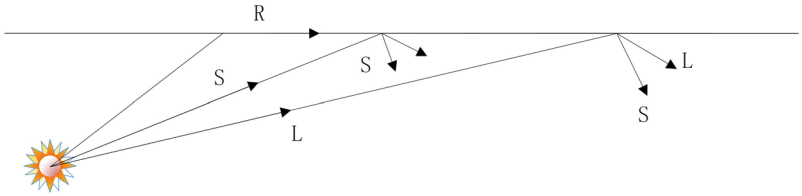

FIG. 8. Wave reflection and mode conversion: O denotes the wave source; L denotes the longitudinal wave; S denotes the shear wave; and R denotes the Rayleigh wave.

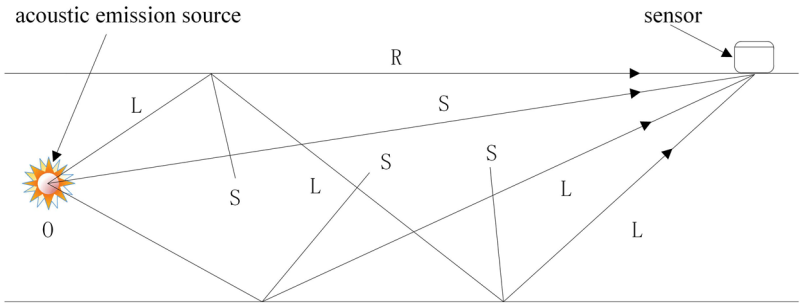

FIG. 9. Wave transmission in thick plate.

concentrations of both the amplitude and energy of the sound signals were found at 0.5 m on the main leg of the KT jacket. If install the sensors at 0.5 m away to the acoustic emission source on the main leg, the acoustic emission signals can be measured stably to ensure the quality of measurements. Because the wave attenuation may concentrate at 0.5 m away to the acoustic emission source, once a crack appear at the joint in the KT jacket, it is possible to detect the damage using the change in attenuation coefficient. As introduced, the energy ratio (E_i/E_s) of rods 1, 3, and 4 stabilized around the value 2, while for rod 2, it was about 1. The corresponding attenuation coefficients calculated from the measured signals were closer to 2 at 0.5 m than those at other distances. Therefore, it is reasonable to place the sensors at 0.5 m away to the joint for each rod.

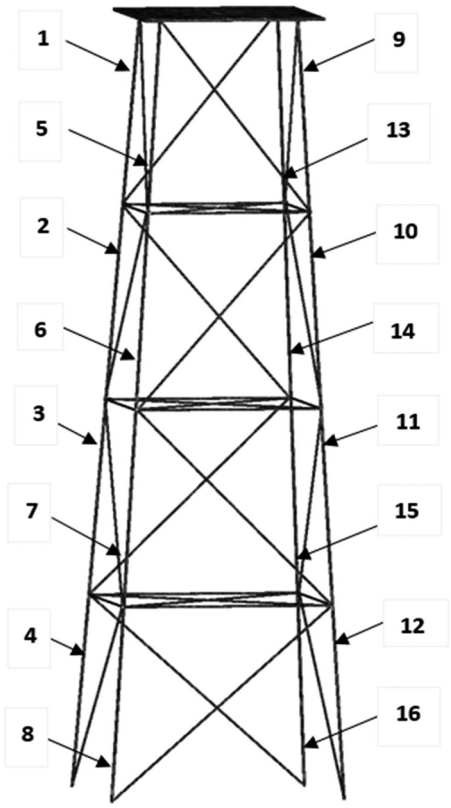

FIG. 10. Sensor layout: the number indicates the sensor's serial number and the arrow indicates the sensor's position.

According to Green's function, the transmission space of the acoustic emission source in the KT jacket can be regarded as a perfect sound field.[29] Its direct sound field is a spherical space, and its reflection reverberation sound field is a complex plane space. Ideally, the acoustic emission wave transmits in the spherical space. However, due to attenuation, in practice, the acoustic emission wave will not transmit in an ideal spherical pattern; but its transmission trend still remains spherical. Hence, in the present research, the measureable radius of the spherical space that the emission source of the joint damage transmits in was 0.5 m. The sensors can be placed at the edge of the spherical space.

Based on the obtained experimental results about the energy attenuation characteristics of the joints, a sensor layout optimization method is proposed for KT-jacket offshore platforms. For each tube joint, the acoustic emission sensors can be installed at 0.5 m position for rods 1, 3, and 4, while for rods 2 and 5, the distance can choose 0.1 m. Figure 10 depicts the optimal sensor layout, where a total 16 sensors are used to monitor the KT-jacket offshore platform, comparing to a number of at least 80 sensors according to theoretical analysis.

III. RESULTS AND DISCUSSIONS

In order to verify the feasibility of the sensor layout optimization method, experimental verification was conducted.

A. Experimental apparatus and procedure

PXR15 sensors with a center frequency of 150 kHz were used in the experimental verification. PXPAIV low-noise amplifier with 40 dB gain was used as the preamplifier. In the

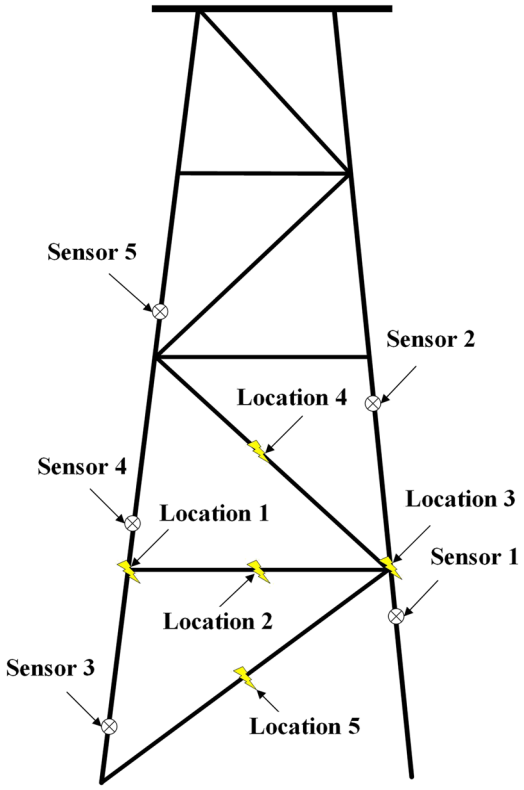

FIG. 11. Sensor layout in sound source positioning experiment.

practical structure, the wave speed was unknown because it is influenced by various factors, such as material type, structural shape, and scale. Therefore, field measurement was carried out to determine the wave speed. The average wave speed in the jacket offshore platform was 3487 m/s. Limited by experimental condition, only five acoustic emission sensors were used in the validation. Figure 11 shows the locations of the jacket joints and sensors. The lead-break simulation test was repeated for five times to analyze the acoustic emission signals.

B. Experimental results

According to the positioning principle of time-difference,[29] the time-difference positioning was implemented using the first two sensors that received the acoustic emission signals. Then, the sound source location can be calculated from the time difference value. Table II lists the sound source positioning error in the experiments.

In Table II, positions 1 and 3 produced the two smallest positioning errors. The maximum error at these two positions was less than 8.0 mm. This is because for position 1 (or 3), sensors 3 and 4 (or 1 and 2) were at 0.5 and 0.1 m away the joint on the same rod. In Table I, it concluded that the measurements within 0.5 m away the sound source was reliable. Thus, the collected signals by sensors 3 and 4 (or 1 and 2) contained accurate information about the location of the acoustic emission source.

TABLE II. Positioning error at different lead-break positions (mm).

Location	Group 1	Group 2	Group 3	Group 4	Group 5	Average
1	2.48	6.82	4.49	3.33	6.82	4.79
2	10.46	13.95	15.11	4.65	4.64	9.76
3	3.645	0.98	6.81	7.99	6.82	5.25
4	6.97	4.65	4.65	9.30	10.466	7.21
5	8.14	8.14	6.97	4.65	8.14	7.21

The positioning errors at positions 2, 4, and 5 in Table II were much larger than these at positions 1 and 3. This is probably because that the actual fatigue damage often occurs at the joints 1 and 3. Therefore, according to Table I, the signals collected at position 2, 4, and 5 may lose useful positioning information. The amplitude and energy curves of the acoustic emission signals emitted from positions 1 and 3 are shown in Figs. 12 and 13. It can be seen from Figs. 12 and 13 that both the amplitude and energy acquired from sensors 3 and 4 (or 1 and 2) were larger than those from sensor 5. These observations were consistent with the results in Table II.

In Fig. 14, the positioning error at positions 2, 4, and 5 is higher than that at positions 1 and 3 in term of the mean value and the maximum value. However, in each experimental test,

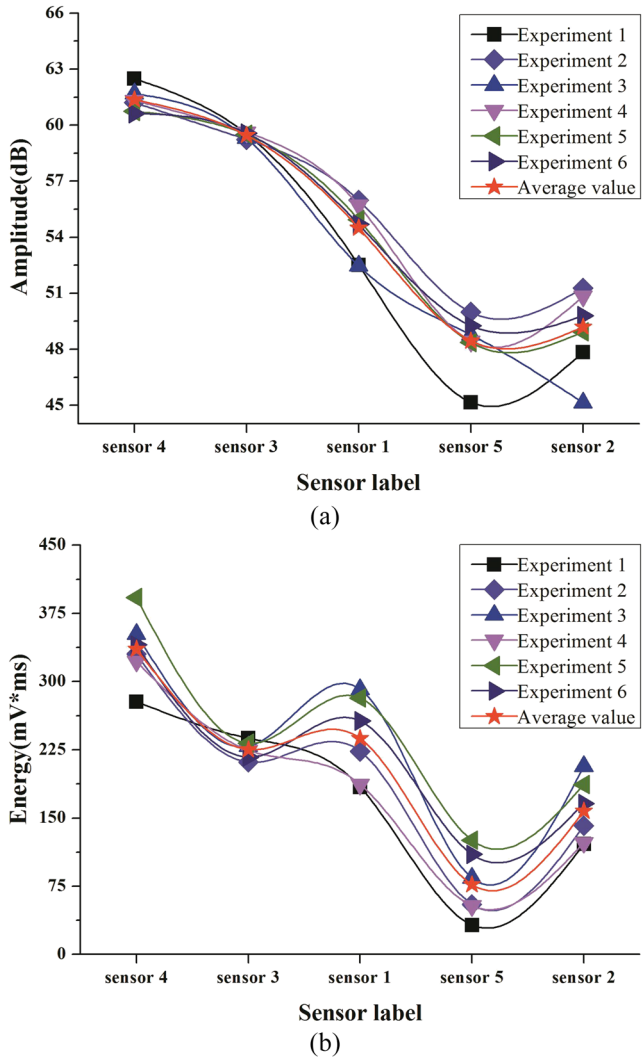

FIG. 12. (a) Amplitude and (b) energy curves obtained from five sensors at position 1.

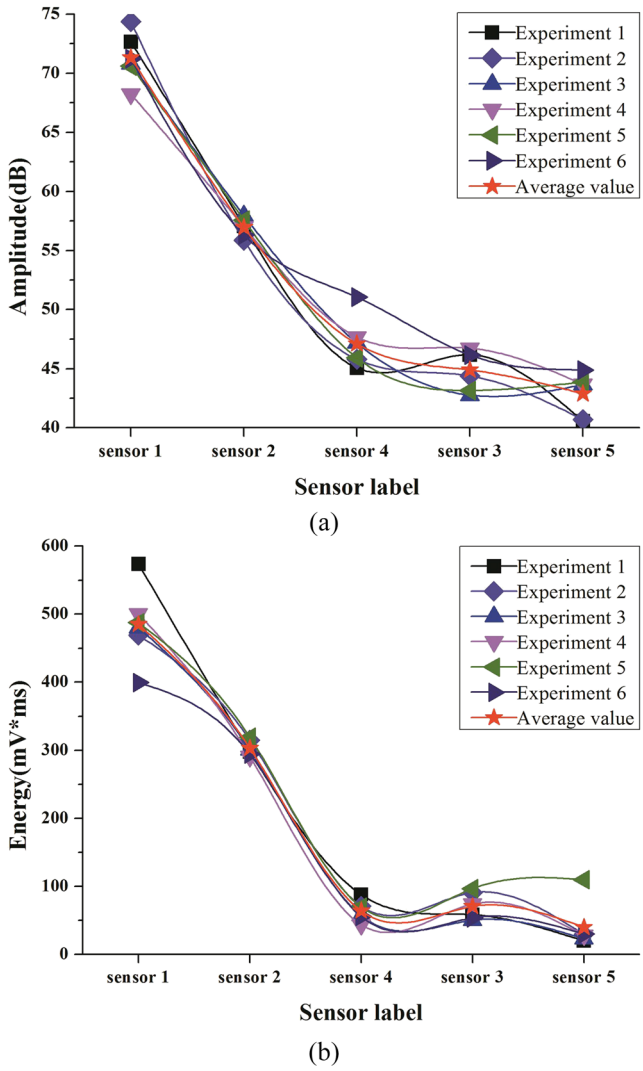

FIG. 13. (a) Amplitude and (b) energy curves obtained from five sensors at position 3.

the positioning errors of positions 1 and 3 were not always the least. The main reason is due to signal fading. For example, the acoustic emission signal generated at joint position 1 will transmit from position 2 to sensors 1 and 4. During this transmission process, the acoustic emission signal will be reflected and its energy will disperse to directions of the jacket supporting rods, causing amplitude and energy attenuation. Furthermore, the test results at positions 2, 4, and 5 demonstrated that the maximum positioning error were less than 15 mm, which was nearly twice of that at positions 1 and 3.

C. Discussions

According to the energy attenuation characteristic test on supporting rods of the KT jacket, the energy attenuation curve of the acoustic emission signal presented a convergence trend at 0.5 m away the sound source. If the acoustic emission signal passes some other joints along supporting rods, the energy attenuation characteristics will change greatly. In order to validate the effectiveness of the proposed sensor layout method, the mean positioning errors were compared with the calculation results in another set of verification tests. Figure 15 manifests the comparison result. The square points in Fig. 15 are the mean positioning errors (see Table II) at each position of the five positions using the proposed sensor layout, while the round points are the mean positioning errors at each position in another set of the verification tests using a different sensor layout (see Table III). Similar test results were obtained, where the mean positioning errors at positions 1 and 3 were the two least.

It is noticed in Fig. 15 that the mean errors of the comparison sensor layout is much larger than that of the proposed sensor layout. This is caused by the energy attenuation of acoustic emission signals after passing through additional joints. As a result, the proposed optimized sensor layout is feasible and reliable for damage detection for the offshore platform.

Actually, the proposed optimized layout of 16 sensors is adequate to identify the acoustic emission sources at all joints in the KT-jacket offshore platform. However, the theoretical analysis requests 80 sensors for the same purpose.

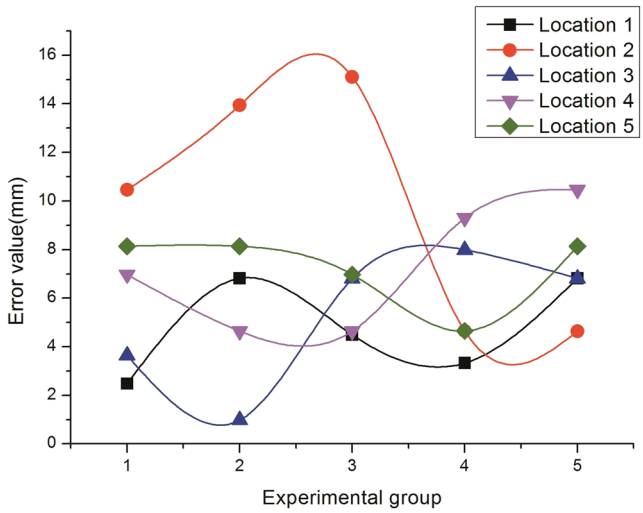

FIG. 14. Positioning test errors at different positions.

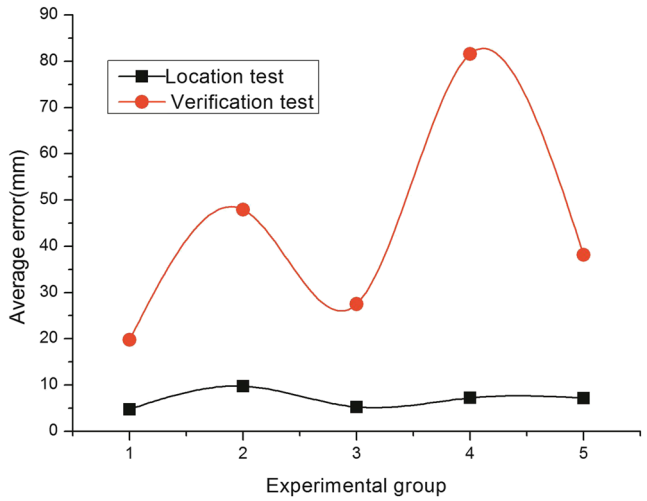

FIG. 15. Mean error of the verification test.

TABLE III. Sensor layout in the verification tests.

	Position 1	Position 2	Position 3	Position 4	Position 5
The proposed sensor layout	3 and 4	1 and 4	1 and 2	1 and 5	1 and 3
The comparison sensor layout	4 and 5	1 and 3	1 and 4	1 and 4	2 and 3

IV. CONCLUSION

This paper proposes an optimal sensor layout for positioning the sound sources in KT jacket offshore platforms, aiming to achieve online damage monitoring with a suitable number of sensors and accurate detection performance. Based on the theoretical analysis on transmission characteristics of acoustic emission wave generated by the cracks in the KT jacket offshore platforms, experimental data were used to determine the optimal layout of the acoustic emission sensors. Sound sources are located through acoustic emission monitoring test. The main conclusions of this paper are drawn as follows.

(1) The attenuation characteristics of the acoustic emission wave on the main leg have been analyzed. Both the amplitude and energy of the acoustic emission signal declined as the wave transmitted away from the sound source. There was evident concentration of the signal amplitude and energy at 0.5 m away from the sound source.
(2) Energy attenuation characteristic test on supporting rods has been analyzed. An experiment study on acoustic emission energy attenuation characteristic is designed for the first time for the KT jacket offshore platform. The analysis results showed that the energy attenuation coefficients at different points away the test joints varied significantly. In addition, the attenuation coefficients at different supporting rods were also different even though the distance to the sound source was the same.
(3) The optimized layout of the acoustic emission sensors based on the energy attenuation characteristics has been conducted. The optimization results demonstrated that only 16 sensors were needed for online damage monitoring, comparing to 80 of the theoretical calculation. In addition, the positioning error of the proposed sensor layout was less than 8 mm. As a result, the sensor layout optimization method has practical importance.

ACKNOWLEDGMENTS

This research was supported by the National Natural Science Foundation of China (No. 51175485), Fundamental Research Funds for the Central Universities (No. 201513043), Shandong Province foundation for Outstanding Young Scientist (No. 2015BSE29009), National Research Foundation, South Africa (No. IFR160118156967 and RDYR160404161474) and UOW VC Fellowship.

[1]N. Habibi, S. M. H. Gangaraj, G. H. Farrahi, G. H. Majzoobi, A. H. Mahmoudi, M. Daghigh, A. Yari, and A. Moridi, "The effect of shot peening on fatigue life of welded tubular joint in offshore structure," Mater. Des. **36**, 250–257 (2012).
[2]H. Qu, Y. F. Hu, J. S. Huo, Y. Z. Liu, and Y. Jiang, "Experimental study on tubular K-joints under impact loadings," J. Constr. Steel Res. **112**, 22–29 (2015).
[3]H. Qu, J. S. Huo, C. Xu, and F. Fu, "Numerical studies on dynamic behavior of tubular T-joint subjected to impact loading," Int. J. Impact Eng. **67**, 12–26 (2014).
[4]F. S. Liu, H. J. Li, W. Li, and D. P. Yang, "Lower-order modal parameters identification for offshore jacket platform using reconstructed responses to a sea test," Appl. Ocean Res. **46**, 124–130 (2014).
[5]Z. Li, Y. Jiang, Q. Guo, C. Hu, and Z. Peng, "Multi-dimensional variational mode decomposition for bearing crack detection in wind turbines with large driving-speed variations," Renewable Energy **116**, 55–73 (2018).
[6]A. Yonezu, H. Cho, and M. Takemoto, "Monitoring of stress corrosion cracking in stainless steel weldments by acoustic and electrochemical measurement," Meas. Sci. Technol. **17**, 2447–2454 (2006).
[7]R. O. Schmidt, "Multiple emitter location and signal parameter estimation," IEEE Trans. Antennas Propag. **34**, 276–280 (1986).
[8]M. Omologo and P. Svaizer, "Acoustic source location in noisy and reverberant environment using CSP analysis," in *Processing of ICASSP* (IEEE, 1996), pp. 921–924.
[9]B. Yegnanarayana, S. Prasanna, R. Duraiswami, and D. Zotkin, "Processing of reverberant speech for time-delay estimation," IEEE Trans. Speech Audio Process. **13**, 1110–1118 (2005).
[10]J. J. Jia, M. J. Liu, and X. F. Li, "Algorithm for acoustic passive localization with dual arrays," Chin. J. Chem. Eng. **21**, 14–17 (2008).
[11]N. H. Faisal and R. Ahmed, "Acoustic emission analysis of Vickers indentation fracture of cermet and ceramic coatings," Meas. Sci. Technol. **22**, 125704 (2011).
[12]S. Ramadan, L. Gaillet, C. Tessier, and H. Idrissi, "Assessment of the stress corrosion cracking in a chloride medium of cables used in prestressed concrete structures by the acoustic emission technique," Meas. Sci. Technol. **19**, 283 (2008).
[13]G. H. Feng, M. Y. Tsai, and Y. R. Jeng, "A micromachined, high signal-to-noise ratio acoustic emission sensor and its application to monitor dynamic wear," Sens. Actuators, A **188**, 56–65 (2012).
[14]T. Lokajicek and K. Klima, "A first arrival identification system of acoustic emission (AE) signals by means of a high-order statistics approach," Meas. Sci. Technol. **17**, 2461–2466 (2006).
[15]M. Meo, "Acoustic emission sensors for assessing and monitoring civil infrastructures," in *Woodhead Publishing Series in Electronic and Optical Materials*, edited by M. L. Wang, J. P. Lynch, and H. Sohn (Woodhead Publishing, 2014), Vol. 55, pp. 159–178, Sensor Technologies for Civil Infrastructures.
[16]Q. Xie, S. Y. Cheng, F. C. Lu, and Y. Q. Li, "A new sparse design method on phased array-based acoustic emission sensor for partial discharge detection," Meas. Sci. Technol. **25**, 035102 (2014).
[17]Q. Xie, X. Liu, J. H. Tao, T. Li, S. Y. Cheng, and F. C. Lu, "Experimental verification of the sparse design of a square partial discharge acoustic emission array sensor," Meas. Sci. Technol. **26**, 045101 (2015).
[18]R. S. Chen, T. Bradshaw, J. Burns, P. Cole, P. Jarman, D. Pedder, R. Theobald, and G. F. Fernando, "Linear location of acoustic emission using a pair of novel fibre optic sensors," Meas. Sci. Technol. **17**, 2313–2318 (2006).
[19]H. Yalcinkaya and D. Ozevin, "The design and calibration of particular geometry piezoelectric acoustic emission transducer for leak detection and localization," Meas. Sci. Technol. **24**, 095103 (2013).
[20]T. Griffin, "Traceability of acoustic emission measurements for a proposed calibration method—Classification of characteristics and identification using signal analysis," Mech. Syst. Signal Process. **50–51**, 757–783 (2015).
[21]T. He, Q. Pan, Y. G. Liu, X. D. Liu, and D. Y. Hu, "Near-field beamforming analysis for acoustic emission source localization," Ultrasonics **52**, 587–592 (2012).
[22]E. D. Niri, A. Farhidzadeh, and S. Salamone, "Determination of the probability zone for acoustic emission source location in cylindrical shell structures," Mech. Syst. Signal Process. **60–61**, 971–985 (2015).
[23]H. Ahmadi and M. A. Lotfollahi-Yaghin, "Stress concentration due to in-plane bending (IPB) loads in ring-stiffened tubular KT-joints of offshore

structures: Parametric study and design formulation," Appl. Ocean Res. **51**, 54–66 (2015).
[24]D. Li and Y. H. Hu, "Energy-based collaborative source localization using acoustic microsensor array," EURASIP J. Appl. Signal Process. **2003**, 985029.
[25]Y. G. Cao, Z. B. Meng, S. H. Zhang, and H. Q. Tian, "FEM study on the stress concentration factors of K-joints with welding residual stress," Appl. Ocean Res. **43**, 195–205 (2013).
[26]G. Li, X. Liu, Y. Liu, and Q. J. Yue, "Optimum design of ice-resistant offshore jacket platforms in the Bohai Gulf in consideration of fatigue life of tubular joints," Ocean Eng. **35**, 484–493 (2008).
[27]A. Gholizad, A. A. Golafshani, and V. Akrami, "Structural reliability of offshore platforms considering fatigue damage and different failure scenarios," Ocean Eng. **46**, 1–8 (2012).
[28]M. Janecek, R. Kral, P. Dobron, F. Chmelik, V. Supik, and F. Hollander, "Mechanisms of plastic deformation in AZ31 magnesium alloy investigated by acoustic emission and transmission electron microscopy," Mater. Sci. Eng., A **462**, 311–315 (2007).
[29]M. G. Baxter, R. Pullin, K. M. Holford, and S. L. Evans, "Delta T source location for acoustic emission," Mech. Syst. Signal Process. **21**, 1512–1520 (2007).